THE NEXT-TO-LEADING ORDER OF THE DIFFERENTIAL CROSS-SECTION OF THE SUBPROCESS OF ANNIHILATION OF QUARK-ANTIQUARK PAIR $q\bar{q} \to g\gamma$ OF PROMPT PHOTON PRODUCTION IN PROTON-PROTON COLLISIONS AT NICA ENERGIES

M.R.Alizada

Department of Theoretical Physics, Baku State University

Z.Khalilov 33, Az-1148 Baku, Azerbaijan, mohsunalizade@gmail.com

INTRODUCTION

The production of prompt photons in proton-proton collisions is an important process for studying the dynamic structure of proton at high energies. Being neutral in color, they have a large mean free path in both dense hadronic matter and quark-gluon plasma (QGP). This allows them to escape from the interaction region unchanged. A photon produced in a proton-proton collision in the energy range from 1.5 to several GeV also carries information about the formation of the QGP, the distribution of partons in nucleons as they are formed, hard scattering of incoming partons such as Compton scattering of quark-gluon, annihilation of quark-antiquark pair, and bremsstrahlung subjected to hard scattering [1, 2, 3].

It is known that the accuracy of theoretical calculations of the prompt photon production depends on the order of the perturbative expansion, which is usually

[1] Aurenche P., Fontannaz M., Guillet J.Ph., Pilon E., Werlen M. Recent critical study of photon production in hadronic collisions // Phys. Rev. D, - 2006. - V. 73. - P. 094007-1 - 094007-10.

[2] Campbell S. Photon production from gluon mediated quark-anti-quark annihilation at confinement // Phys. Rev. C, - 2015. – V. 92, - P. 014907-1 – 014907-10.

[3] Martina A.D., Stirlingb W.J., Thornec R.S., Wattc G. Parton distributions for the LHC // Eur. Phys. J. C - 2009, - V. 63, - P. 189 -285.

expressed in terms of the strong coupling constant α_s. The leading order (LO) approximation, which corresponds to the lowest power of strong coupling α_s, is often insufficient to describe the experimental data, especially at large transverse momenta of photons p_T. Therefore, it is necessary to use higher-order corrections, such as next-to-leading order (NLO), next-to-next-to-leading order (NNLO), which take into account the effects of one-loop virtual diagrams and real production of additional particles [4, 5, 6, 7, 8, 9, 10].

[4] Gordon L.E., Vogelsangt W. Isolated prompt photon production at DESY HERA // Phys. Rev. D 1995, V, 52, no 1, -P. 58-67.
[5] Elaf M. Mohammed, Hadi J.M. Al-Agealy, Nada Farhan Kadhim Theoretical and calculation the photon production from quark-antiquark interaction // Educational and Scientific Studies - College of Education - The Iraqi University, Physics Sciences, December 2022) DOI: 10.52866/esj.2021.05.20.07.
[6] Stremmer D., Worek M. Complete NLO corrections to top-quark pair production with isolated photons // arXiv:2403.03796v2 [hep-ph] 16 Jul 2024.
[7] Florian König Prompt Photon Production Predictions at NLO and in POWHEG Inaugural-Dissertation for the degree of Doctor of Natural Sciences, Faculty of Mathematics and Natural Sciences, Westfälische Wilhelms-Universität Münster, 2016.
[8] Matthew D. S. Precision direct photon spectra at high energy and comparison to the 8 TeV ATLAS data // JHEP, 2016, V.09, P.005.
[9] Chen X., Gehrmann T., Glover E.W.N, Höfer M., Huss A., Schürmann R. Single Photon Production at Hadron Colliders at NNLO QCD with Realistic Photon Isolation // arXiv:2205.01516v1 [hep-ph] 3 May 2022.
[10] Baer H., Ohnemus J., Owens J.F. Next-to-leading-logarithm calculation of prompt photon production // Phys.Rev. D - 1990, - V. 42, n. 1, - P.61-71.

Research into the production of prompt photons in proton-proton collisions at the Nuclotron-based Ion Collider fAcility, i.e. NICA, energies has its advantages. The energy of NICA (10 GeV) does not allow the production of many elementary particles, which makes it difficult to accurately determine the differential cross-section of prompt photons production, and will also help determine the temperature of the phase transition to quark-gluon plasma and hadronization [11, 12].

At early, we investigated prompt photon production in Compton scattering of quark-gluon $qg \to q\gamma$, annihilation of quark-antiquark pair $q\bar{q} \to g\gamma$ and bremsstrahlung of quarks $qq \to qq\gamma$ in collision of nonpolarized, and logitudinally polarized proton in LO at $\sqrt{s}$=10 GeV, NICA energies [13, 14, 15, 16]. It has been shown, differential cross section of

---

[11] Kekelidze V. D. Heavy ion collision experiments at NICA // PEPAN Letter, 2018. V. 49. P. 827-851.
[12] Arbuzov A.B., Bacchetta A., Butenschoend M., Celiberto F.G., and et al. On the physics potential to study the gluon content of proton and deuteron at NICA SPD // Prog. Part. Nucl. Phys., - 2021. Feb; - V. 119. - P. 1-48.
[13] Alizada M.R., Ahmadov A.I., Arbuzov A.B. Prompt photon production in subprocesses $qg \to q\gamma$ and $q\gamma \to q\gamma$ of Compton scattering in proton-proton collision at NICA energies // Physics of Particles and Nucleer Letters, - 2024, - 21(2), - P. 85–89.
[14] Alizada M.R. Abstract of thesis of "Description of prompt photon production in proton-proton collision at NICA energies" // https://aak.gov.az/upload/dissertasion/fizika/AVTOREFERAT__ALIZADE__MR___AZERB1.pdf].
[15] Nishijima K. Generalized Furry's theorem for closed loops // Progress of Theoretical Physics, - V. 6, No4, August - 1951, - P, 614–615.

prompt photons production consists of more than 50% of the differential cross-section of the subprocess of Compton scattering of quark-gluon and about 43% of the differential cross-section of annihilation of quark-antiquark pairs and less than 0.03% of the differential cross-section of bremsstrahlung. Despite the low collision energies, Compton scattering of quark-gluon $qg \to g\gamma$ remains dominant, as in LHC, American Tevatron energies. The difference is that Compton scattering at LHC energies, American Tevatron 95% of the total cross-section production of prompt photons. We also have shown that, the prompt photons produced in pure electrodynamics Compton scattering constitute 10% of the prompt photons produced in mixed Compton scattering [16].

In this presentation, we present result of the study of prompt photon production in annihilation of quark-antiquark pair in the NLO approximation at collision of nonpolarized and the longitudinally polarized protons at NICA energies, and compares with calculations in LO.

---

[16] Owens J.F. Large-momentum-transfer production of direct photons, jets, and particles // Reviews of Modern Physics. - 1987, - V. 59, - P. 465-503.

II. DIFFERENTIAL CROSS-SECTION OF ONE-LOOP CORRECTIONS TO THE SUBPROCESS OF ANNIHILATION OF QUARK-ANTIQUARK PAIR $q\bar{q} \to g\gamma$

We used FeynCalc for generation of Feynman diagrams of the subprocess of annihilation of quark-antiquark pairs $q\bar{q} \to g\gamma$ in NLO. In this case 773 one-loop diagrams were generated. Among the diagrams, the ones with heavy particles (H, G, Z, W, t, c, b, μ, τ, e), which are not registered at NICA SPD, the ones with triangular loops of fermions and vector bosons, which vanish by the Furry theorem [16], the ones with "seagulls" and the ones with loops on external legs, which are excluded in the renormalization scheme on the mass shell, as well as the ones with photon-gluon transitions, which do not conserve color, were not taken into account. As a result, we obtained the following 12 diagrams, which contribute to the prompt photons production in NLO at NICA energies (Figure 1).

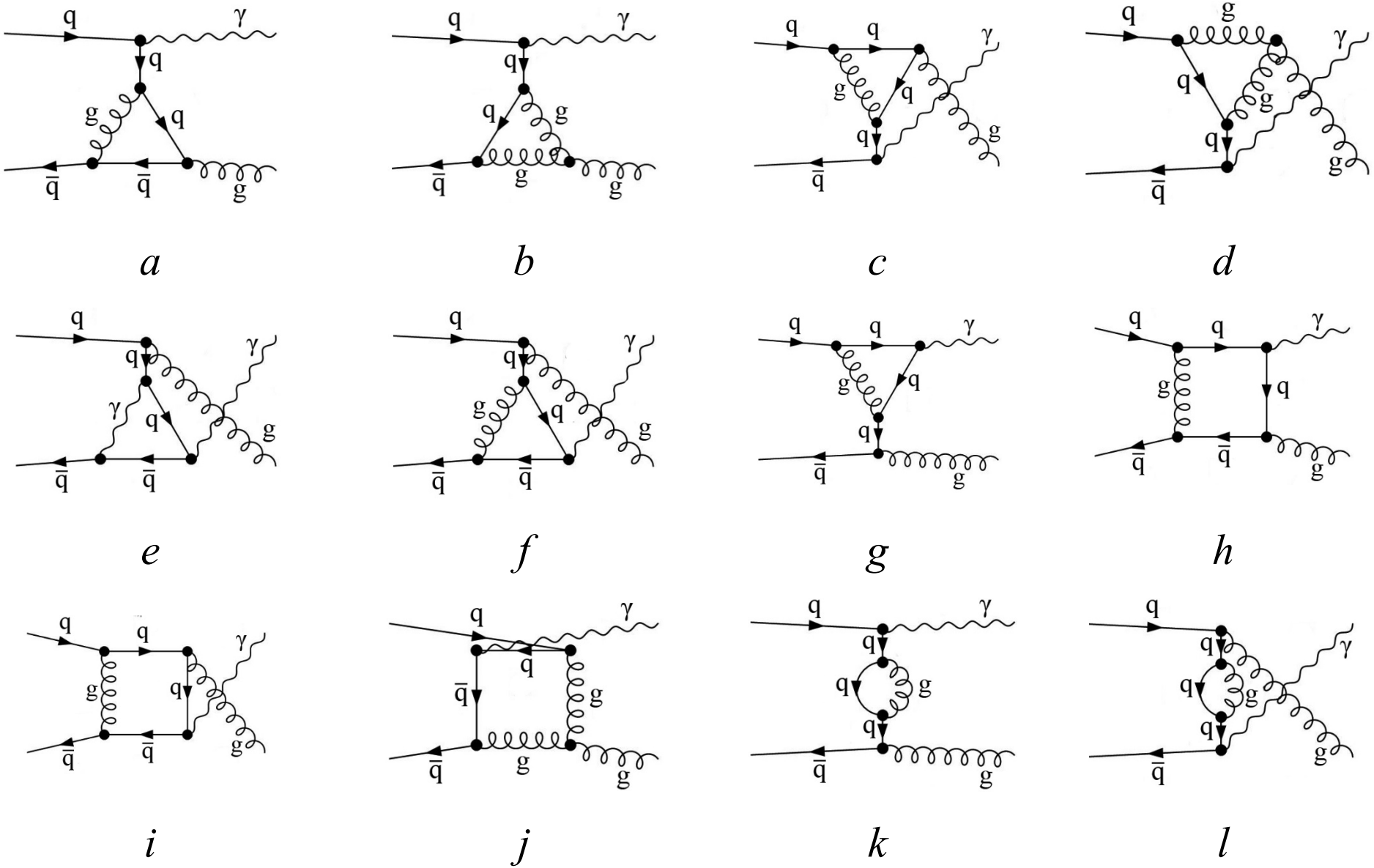

Fig.1(a,b,c,d,e,f,g,h,i,j,k,l). Feynman diagrams of the one-loop corrections to the subprocess of annihilation of quark-antiquark pair $q\bar{q} \to g\gamma$

NLO calculation has been carried out using dimensional regularization and the Minimal Supersymmetric Standard Model (MSSM) scheme [16].

In the parton level the Mandelstam invariants of subprocess $q(p_1)+\bar{q}(p_2)\to g(k_1)+\gamma(k_2)$ in LO and NLO is same: $\hat{s}=(p_1+p_2)^2$, $\hat{t}=(p_1-k_1)^2$ and $\hat{u}=(p_2-k_1)^2$.

Matrix elements of processes in NLO are:

$$M_1=\frac{-iee_q g_s^3 T^{Glu5}_{Col6Col1}T^{Glu5}_{Col2Col5}T^{Glu4}_{Col5Col6}\bar{v}(p_2)\gamma\hat{q}\hat{\varepsilon}^*(k_1)(\hat{k}_1-\hat{q})\gamma(\hat{k}_1-\hat{p}_2)\hat{\varepsilon}^*(k_1)u(p_1)}{144\pi^4 q^2(p_2-k_1)^2(q-p_2)^2(q-k_1)^2},$$

$$M_2=\frac{ee_q g_s^3 T^{Glu6}_{Col5Col1}T^{Glu5}_{Col2Col5}f^{Glu4Glu5Glu6}\left(k_1\varepsilon^*(k_1)-2q\varepsilon^*(k_1)\right)\bar{v}(p_2)\gamma(\hat{q}-\hat{p}_2)\gamma\left(\hat{k}_1+\hat{p}_2\right)\hat{\varepsilon}^*(k_2)u(p_1)}{144\pi^4 q^2(p_2-k_1)^2(q-p_2)^2(q-k_1)^2}+$$

$$+\frac{ee_q g_s^3 T^{Glu6}_{Col5Col1}T^{Glu5}_{Col2Col5}f^{Glu4Glu5Glu6}\bar{v}(p_2)\left(\hat{q}-2\hat{k}_1\right)(\hat{q}-\hat{p}_2)\hat{\varepsilon}^*(k_1)\left(\hat{k}_1-\hat{p}_2\right)\hat{\varepsilon}^*(k_2)u(p_1)}{144\pi^4 q^2(p_2-k_1)^2(q-p_2)^2(q-k_1)^2}+$$

$$+\frac{ee_q g_s^3 T^{Glu6}_{Col5Col1}T^{Glu5}_{Col2Col5}f^{Glu1Glu5Glu6}\bar{v}(p_2)\hat{\varepsilon}^*(k_1)(\hat{q}-\hat{p}_2)(\hat{k}_1+\hat{q})(\hat{k}_1-\hat{p}_2)\hat{\varepsilon}^*(k_2)u(p_1)}{144\pi^4 q^2(p_2-k_1)^2(q-p_2)^2(q-k_1)^2},$$

$$M_3=\frac{iee_q g_s^3 T^{Glu5}_{Col5Col1}T^{Glu5}_{Col2Col6}T^{Glu4}_{Col6Col5}\bar{v}(p_2)\hat{\varepsilon}^*(k_2)(\hat{k}_2-\hat{p}_2)\gamma(\hat{q}-\hat{k}_1)\hat{\varepsilon}^*(k_1)\hat{q}\gamma u(p_1)}{144\pi^4 q^2(p_2-k_2)^2(q-p_2)^2(q-k_1)^2(p_2-k_1-k_2+q)^2},$$

$$M_4=\frac{ee_q g_s^3 T^{Glu5}_{Col5Col1}T^{Glu6}_{Col2Col5}f^{Glu4Glu5Glu6}(k_1\varepsilon^*(k_1)-2q\varepsilon^*(k_1))\bar{v}(p_2)\hat{\varepsilon}^*(k_2)(\hat{k}_2-\hat{p}_2)\gamma(\hat{k}_1+\hat{k}_2-\hat{p}_2-\hat{q})\gamma u(p_1)}{144\pi^4 q^2(p_2-k_2)^2(q-k_1)^2(p_2+q-k_1-k_2)^2}+$$

$$+\frac{ee_q g_s^3 T^{Glu6}_{Col5Col1} T^{Glu5}_{Col2Col5} f^{Glu4Glu5Glu6} \bar{v}(p_2)\left(\hat{q}-2\hat{k}_1\right)(\hat{q}-\hat{p}_2)\hat{\varepsilon}^*(k_1)\left(\hat{k}_1-\hat{p}_2\right)\hat{\varepsilon}^*(k_2)u(p_1)}{144\pi^4 q^2(p_2-k_2)^2(q-k_1)^2(p_2+q-k_1-k_2)^2}+$$

$$+\frac{ee_q g_s^3 T^{Glu6}_{Col5Col1} T^{Glu5}_{Col2Col5} f^{Glu1Glu5Glu6} \bar{v}(p_2)\hat{\varepsilon}^*(k_1)(\hat{q}-\hat{p}_2)\left(\hat{k}_1+\hat{q}\right)\left(\hat{k}_1-\hat{p}_2\right)\hat{\varepsilon}^*(k_2)u(p_1)}{144\pi^4 q^2(p_2-k_2)^2(q-k_1)^2(p_2+q-k_1-k_2)^2},$$

$$M_5=\frac{-ie^3 e_q g_s T^{Glu5}_{Col2Col1} \bar{v}(p_2)\gamma\hat{q}\hat{\varepsilon}^*(k_2)\left(\hat{k}_2-\hat{q}\right)\gamma\left(\hat{k}_2-\hat{p}_2\right)\hat{\varepsilon}^*(k_1)u(p_1)}{324\pi^4 q^2(p_2-k_2)^2(q-p_2)^2(q-k_2)^2},$$

$$M_6=\frac{-iee_q g_s^3 T^{Glu4}_{Col5Col1} T^{Glu4}_{Col2Col6} T^{Glu5}_{Col6Col5} \bar{v}(p_2)\gamma\hat{q}\hat{\varepsilon}^*(k_2)\left(\hat{k}_2-\hat{q}\right)\gamma\left(\hat{k}_2-\hat{p}_2\right)\hat{\varepsilon}^*(k_1)u(p_1)}{144\pi^4 q^2(p_2-k_2)^2(q-p_2)^2(q-k_2)^2},$$

$$M_7=\frac{iee_q g_s^3 T^{Glu5}_{Col6Col1} T^{Glu4}_{Col2Col5} T^{Glu5}_{Col5Col6} \bar{v}(p_2)\hat{\varepsilon}^*(k_1)\left(\hat{k}_1-\hat{p}_2\right)\gamma\left(\hat{q}-\hat{k}_2\right)\hat{\varepsilon}^*(k_2)\hat{q}\gamma u(p_1)}{144\pi^4 q^2(p_2-k_1)^2(q-k_2)^2(p_2+q-k_1-k_2)^2},$$

$$M_8=\frac{-iee_q g_s^3 T^{Glu5}_{Col5Col1} T^{Glu5}_{Col2Col6} T^{Glu4}_{Col6Col5} \bar{v}(p_2)\gamma(\hat{q}+\hat{p}_2)\hat{\varepsilon}^*(k_1)\left(\hat{k}_1-\hat{p}_2-\hat{q}\right)\hat{\varepsilon}^*(k_2)\left(\hat{k}_1+\hat{k}_2-\hat{p}_2-\hat{q}\right)\gamma u(p_1)}{144\pi^4 q^2(p_2+q)^2(q+p_2-k_1)^2(p_2+q-k_1-k_2)^2},$$

$$M_9=\frac{-iee_q g_s^3 T^{Glu5}_{Col5Col1} T^{Glu5}_{Col2Col6} T^{Glu4}_{Col6Col5} \bar{v}(p_2)\gamma(\hat{q}+\hat{p}_2)\hat{\varepsilon}^*(k_2)\left(\hat{k}_2-\hat{p}_2-\hat{q}\right)\hat{\varepsilon}^*(k_1)\left(\hat{k}_1+\hat{k}_2-\hat{p}_2-\hat{q}\right)\gamma u(p_1)}{144\pi^4 q^2(p_2+q)^2(q+p_2-k_2)^2(p_2+q-k_1-k_2)^2},$$

$$M_{10}=\frac{ee_q g_s^3 T^{Glu5}_{Col5Col1} T^{Glu6}_{Col2Col5} f^{Glu4Glu5Glu6}\left(2p_2\varepsilon^*(k_1)-k_1\varepsilon^*(k_1)-2k_2\varepsilon^*(k_1)+2q\varepsilon^*(k_1)\right)\bar{v}(p_2)\gamma\left(\hat{q}-\hat{k}_2\right)\hat{\varepsilon}^*(k_2)\hat{q}\gamma u(p_1)}{144\pi^4 q^2(q-k_2)^2(p_2-k_2+q)^2(p_2+q-k_1-k_2)^2}$$

$$+\frac{ee_q g_s^3 T^{Glu5}_{Col5Col1} T^{Glu6}_{Col2Col5} f^{Glu4Glu5Glu6} \bar{v}(p_2)\left(2\hat{k}_1+\hat{k}_2-\hat{p}_2-\hat{q}\right)\left(\hat{q}-\hat{k}_2\right)\hat{\varepsilon}^*(k_2)\hat{q}\hat{\varepsilon}^*(k_1)u(p_1)}{144\pi^4 q^2(q-k_2)^2(p_2-k_2+q)^2(p_2+q-k_1-k_2)^2}+$$

$$+\frac{ee_q g_s^3 T^{Glu5}_{Col5Col1} T^{Glu6}_{Col2Col5} f^{Glu4Glu5Glu6} \bar{v}(p_2)\hat{\varepsilon}^*(k_1)\left(\hat{q}-\hat{k}_2\right)\hat{\varepsilon}^*(k_2)\hat{q}\left(\hat{k}_2-\hat{k}_1-\hat{p}_2-\hat{q}\right)u(p_1)}{144\pi^4 q^2(q-k_2)^2(p_2-k_2+q)^2(p_2+q-k_1-k_2)^2},$$

$$M_{11}=\frac{iee_q g_s^3 T^{Glu5}_{Col6Col1} T^{Glu4}_{Col2Col5} T^{Glu5}_{Col5Col6} \bar{v}(p_2)\hat{\varepsilon}^*(k_1)\left(\hat{k}_1-\hat{p}_2\right)\gamma\hat{q}\gamma\left(\hat{k}_1-\hat{p}_2\right)\hat{\varepsilon}^*(k_2)u(p_1)}{144\pi^4 q^2(p_2-k_1)^4(p_2+q-k_1)^2},$$

$$M_{12}=\frac{iee_q g_s^3 T^{Glu4}_{Col5Col1} T^{Glu5}_{Col2Col6} T^{Glu5}_{Col6Col5} \bar{v}(p_2)\hat{\varepsilon}^*(k_2)\left(\hat{k}_2-\hat{p}_2\right)\gamma\hat{q}\gamma\left(\hat{k}_2-\hat{p}_2\right)\hat{\varepsilon}^*(k_1)u(p_1)}{144\pi^4 q^2(p_2-k_2)^4(p_2+q-k_2)^2}.$$

The square of the modulus of the matrix elements for the one-loop correction subprocess $q\bar{q} \to g\gamma$, with applied dimensional regularization and averaged over the spin of the initial particles, has the form:

$$|\bar{M}|^2 = -\frac{\alpha_s e^2 e_q^2 (\alpha_s^2 (0.0004\hat{s}^2 + 0.0008\hat{s}\hat{t} + 0.0008\hat{t}^2) + 0.001\alpha_s \hat{s}^2\hat{t}^2 + 0.0006\hat{s}^2\hat{t}^2)}{\hat{t}(\hat{s} + \hat{t})}.$$

where α_s - is the strong coupling constant at the factorization scale, which we choose equal to $\hat{s}$, e_q - is the electric charge of the quark.

The differential cross-section of the subprocess in parton level was defined as in [16]:

$$\frac{d\hat{\sigma}_{NLO}(q\bar{q} \to g\gamma)}{d\hat{t}} = -\frac{\alpha_s e^2 e_q^2 (\alpha_s^2 (0.0004\hat{s}^2 + 0.0008\hat{s}\hat{t} + 0.0008\hat{t}^2) + 0.001\alpha_s \hat{s}^2\hat{t}^2 + 0.0006\hat{s}^2\hat{t}^2)}{16\pi\hat{s}^2\hat{t}(\hat{s} + \hat{t})}.$$

To calculate the differential cross-section at the hadron level, we used the parton distribution functions (PDF) in NLO level: $G_{q_1/h_1}(x_1)$ and $G_{q_2/h_2}(x_2)$ in accordance with [16] at the factorization scale $\hat{s}$:

$$d\sigma = \int d\hat{\sigma} \cdot G_{q_1/h_1}(x_1) G_{q_2/h_2}(x_2) dx_1 dx_2.$$

In particular, for the differential distributions by rapidity and square of transverse momentum, we obtain the following expressions:

$$\frac{d\sigma}{dy} = \int (-t) G_{q_i/h_1}(x_1) G_{q_i/h_2}(x_2) dx_1 dx_2 \frac{d\hat{\sigma}}{d\hat{t}} +$$

$$+ \int (-t) G_{q_i/h_2}(x_1) G_{q_i/h_1}(x_2) dx_1 dx_2 \frac{d\hat{\sigma}}{d\hat{t}} =$$

$$= \int (-t) \left[G_{q_i/h_1}(x_1) G_{q_i/h_2}(x_2) + G_{q_i/h_2}(x_1) G_{q_i/h_1}(x_2) \right] dx_1 dx_2 \frac{d\hat{\sigma}}{d\hat{t}} =$$

$$= \int (-t) P_{q\bar{q}} dx_1 dx_2 \frac{d\hat{\sigma}}{d\hat{t}}$$

where

$$P_{q\bar{q}} = \sum_{i=1}^{n} e_{q_i}^2 \left[G_{q_i/h_1}(x_1) G_{q_i/h_2}(x_2) + G_{q_i/h_2}(x_1) G_{q_i/h_1}(x_2) \right].$$

and

$$\frac{d\sigma}{dp_T^2} = \int \left(\frac{-t}{2p_T^2} \right) G_{q_1/h_1}(x_1) G_{q_2/h_2}(x_2) dx_1 dx_2 \frac{d\hat{\sigma}}{d\hat{t}}$$

In a similar way we obtain $d\sigma/dx_T^2$ и $d\sigma/dCos(\theta)$.

$$\frac{d\sigma}{dx_T^2} = \int dx_1 dx_2 \, G_{q_1/h_1}(x_1) \, G_{q_2/h_2}(x_2) \, \frac{d\hat{\sigma}}{d\hat{t}} \, \frac{\hat{s}}{4|Cos(\theta)|}$$

$$\frac{d\sigma}{d\cos\theta} = \int dx_1 dx_2 \, G_{q_1/h_1}(x_1) \, G_{q_2/h_2}(x_2) \, \frac{d\hat{\sigma}}{d\hat{t}} \, \frac{\hat{s}}{2}$$

The longitudinal polarization of colliding quarks and antiquarks is taken into account as in [17]:

$$U(p_1)\bar{U}(p_1) = \frac{1}{2}(1 - \lambda_1\gamma_5)(\hat{p}_1 + m_1),$$

$$v(p_2)\bar{v}(p_2) = \frac{1}{2}(1 + \lambda_2\gamma_5)(\hat{p}_2 + m_2),$$

where λ_1 и λ_2 helicity of colliing protons, m_1, m_2 mass of quark and antiquark, p_1, p_2 - transverse momentum of quark and antiquark, correspondingly.

To calculation of the differential cross section of processes with longitudinally polarized colliding protons a polarized PDF was used as in [18]:

$$\Delta u_v(x, Q_0^2) = x^{-0.441} \cdot (1 - x)^{3.96} \cdot (0.928 + 0.149 \cdot x^{0.5} - 1.141 \cdot x + 11.612 \cdot x^{1.5})$$

[17] Okun L.B. Leptoni i kvarki - Moscow, Nauka, 1990, 345p.
[18] Cheng H-Y., Hsiang H. L., Wu C-Yi. Polarized parton distribution functions revisited // Phys. Rev. D 53 - 1996, -P. 2380-2389.

$$\Delta d_v(x, Q_0^2) = x^{-0.665} \cdot (1-x)^{4.46} \cdot (-0.038 - 0.43 \cdot x^{0.5} - 5.260 \cdot x + 8.443 \cdot x^{1.5})$$

$$\Delta G(x, Q_0^2) = x^{-1.17} \cdot (1-x)^{5.33} \cdot (0.03 - 1.71 \cdot x^{0.5} + 3.01 \cdot x + 43.5 \cdot x^{1.5})$$

It is known that the fraction of photon-type partons in a proton can be comparable to the fraction of sea quarks at large values x. The distribution of polarized photons in the proton was taken into account as in [17, 19]:

$$G_{\gamma/p}(x, Q_0) = \frac{\alpha_\gamma}{2\pi}\left(A_u e_u^2 \tilde{P}_{\gamma q} \otimes u(x) + A_d e_d^2 \tilde{P}_{\gamma q} \otimes d(x)\right),$$

where: $A_i = \ln\left(\frac{Q_0^2}{m_i^2}\right)$, $\tilde{P}_{\gamma q} = \frac{1+(1-z)^2}{z}$ - splitting function, Q_0 - factorization scale.

The matrix elements and Mandelstam invariants of the process of production of

[19] Kanazawa, Y., Koike Y., Nishiyama N. A_{LT} in the polarized Drell-Yan process at RHIC and HERA energies // Phys. Lett. B, - 1998. - V. 430. - P. 195-202.

prompt photons in the subprocess of annihilation of the quark-antiquark pair $q\bar{q} \to g\gamma$ studied in the NLO will remain unchanged, as for the case without polarization.

For the square of the matrix element averaged over the spin of the initial particles in the case of one-loop correction of the subprocess $q\bar{q} \to g\gamma$, applying dimensional regularization, we obtain:

$$|\bar{M}|^2 = -\frac{\alpha_s e^2 e_q^2 (1-\lambda_1\lambda_2)(\alpha_s^2(0.0004\hat{s}^2 + 0.0008\hat{s}\hat{t} + 0.0008\hat{t}^2) + 0.001\alpha_s\hat{s}^2\hat{t}^2 + 0.0006\hat{s}^2\hat{t}^2)}{\hat{t}(\hat{s}+\hat{t})}.$$

For the differential cross section of the subprocess $q\bar{q} \to g\gamma$ at the parton level, taking into account the longitudinal polarization of protons, it was obtained as:

$$\frac{d\hat{\sigma}_{NLO}(q\bar{q} \to g\gamma)}{d\hat{t}} = \frac{1}{16\pi\hat{s}^2}\,|\bar{M}|^2.$$

To calculate the differential cross-section at the hadron level, it is necessary to take into account the polarized PDFs for the NLO in the calculations.

Doublespin asymmetry of subprocesses $q\bar{q} \to g\gamma$ has been calculated as in [19]:

$$A_{LL} = \frac{\sigma^{\uparrow\uparrow} - \sigma^{\uparrow\downarrow}}{\sigma^{\uparrow\uparrow} + \sigma^{\uparrow\downarrow}}$$

where $\sigma^{\uparrow\uparrow}$ и $\sigma^{\uparrow\downarrow}$ - cross sections of processes calculated with, respectively, directed and oppositely directed polarizations of colliding protons.

Doublespin asymmetry of subprocesses $q\bar{q} \to g\gamma$ in parton level is obtained:

$$\hat{A}_{LL} = -\lambda_1\lambda_2.$$

As can be seen, A_{LL} is determined by the product of the helicities of the initial particles.

To compare differential cross sections at the parton level, calculated in the LO and NLO approximations, we used the relation $\hat{R} = \frac{d\hat{\sigma}_{NLO}}{d\hat{\sigma}_{LO}}$ and find the following expression $\hat{R} \approx 0.005\alpha_s$. The hadron level relationship $R = \frac{d\sigma_{NLO}}{d\sigma_{LO}}$ is determined using PDF. Investigation of the dependence of the ratio $R = \frac{d\sigma_{NLO}}{d\sigma_{LO}}$ on the total energy of colliding particles $\sqrt{s}$, the transverse momentum p_T of produced photons, the cosine of scattering angle and rapidity y of photon has been carried out.

Study of the polarization effects of colliding protons on the differential cross-section of the process of prompt photons production by determining the $R = \frac{d\sigma_{NLO,POL}}{d\sigma_{NLO}}$ ratio.

III. NUMERICAL RESULTS AND THEIR DISCUSSION

a. Differential cross-section of subprocess of annihilation of quark-antiquark pair $q\bar{q} \to g\gamma$ *at collision of nonpolarized protons*

Figure 2(a,b,c,d,e) shows the dependence of the differential cross section of the subprocess $q\bar{q} \to g\gamma$, calculated in the NLO, on the sum of the energy of colliding particles $\sqrt{s}$, the transverse momentum of prompt photons p_T, the cosine of the scattering angle Cos(θ) of prompt photons, the rapidity y (d) and x_T (d) at $\sqrt{s}$=10 GeV. In this case, restrictions are imposed on the transverse momentum $p_T \geq 0.5$ GeV/c and the rapidity of prompt photons $-2 \leq y \leq 2$.

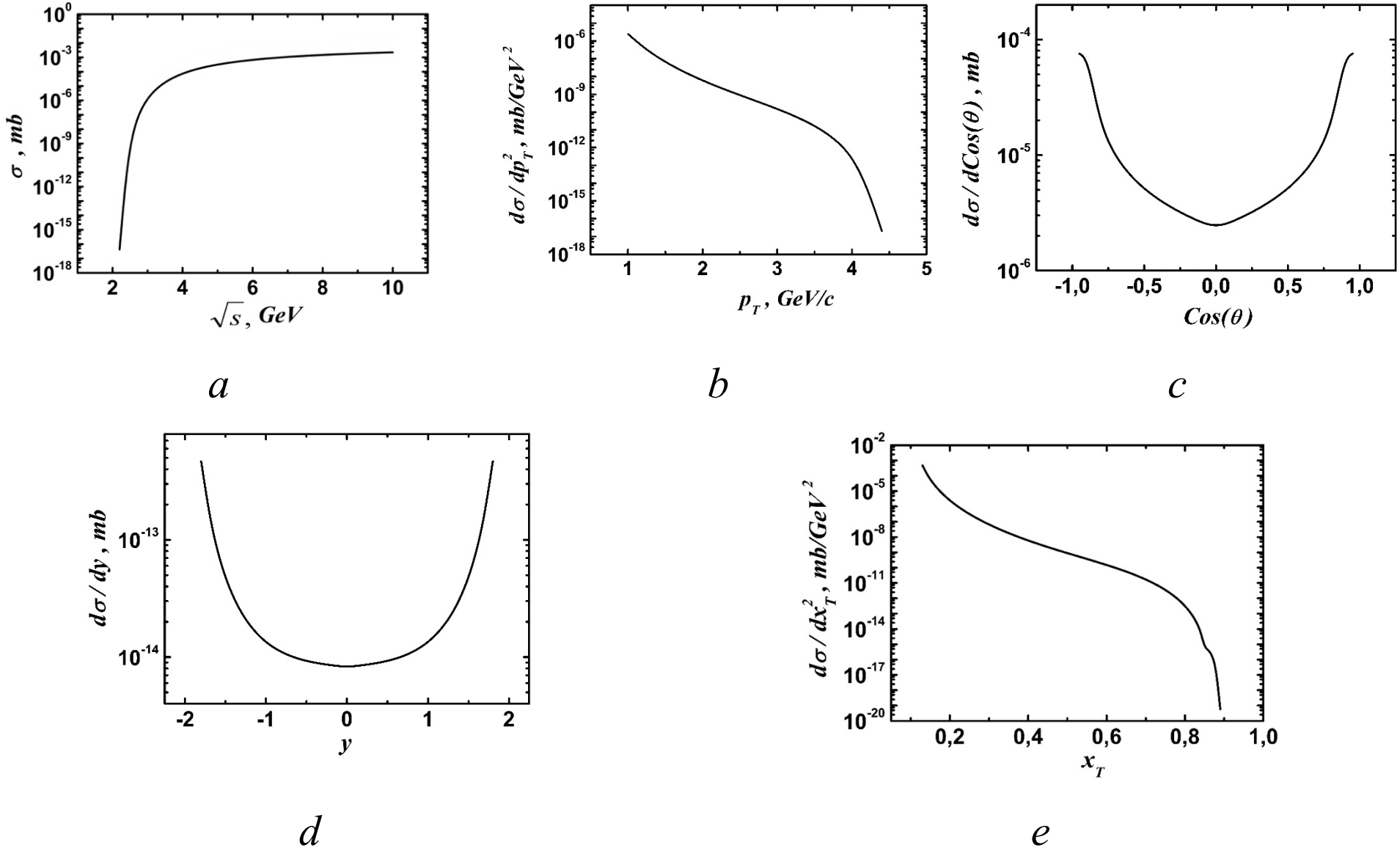

Figure 2(a,b,c,d,e). The dependence of the differential cross section of the subprocess $q\bar{q} \to g\gamma$, calculated in the NLO, on the sum of the energy of colliding particles $\sqrt{s}$, the transverse momentum of prompt photons p_T, the cosine of the scattering angle Cos(θ) of prompt photons, the rapidity y (d) and x_T (d) at $\sqrt{s}$=10 GeV.

It can be seen from Figure 2(a) that at low energies the total cross section increases rapidly with the increase in the value of $\sqrt{s}$. The total cross-section reaches a maximum at the value $\sqrt{s}$=5.2 GeV, and then slowly decreases with further growth of the value $\sqrt{s}$. We assume that at low energies, quarks and antiquarks have a small relative velocity and, therefore, strongly overlap in space and time. This increases the probability of gluon and photon emission, which have no mass and can carry most of the energy. The cross section is proportional to the square of the electric charge of the quark. Consequently, the differential cross section for upper quarks is greater than for lower quarks. The differential cross-section is also suppressed by the running coupling constant α_s QCD, which decreases with the growth of energy. Therefore, the differential cross section for higher energies is smaller than for lower energies.

As can be seen from Figure 2(b), the differential cross section $d\sigma/dp_T^2$ decreases sharply with increasing p_T. This is because the production of high-p_T particles requires

more energy and is suppressed by the running QCD coupling constant, which decreases with increasing energy scale. In addition, such a rapid decrease is characteristic of hard scattering processes such as quark-antiquark pair annihilation, due to the increase in phase space available for particles in the higher-momentum final state.

The dependence of the differential cross section $d\sigma/dCos(\theta)$ on the scattering angle cosine Cos(θ) has a symmetrical peaked shape with a maximum at Cos(θ)=±1 and a minimum at Cos(θ)=0 (Figure 2(c)). This is due to the fact that the $q\bar{q} \rightarrow g\gamma$ subprocess is dominated by the t-channel exchange of a virtual photon, which has spin 1 and an even-even nature. The angular distribution of the final state particles reflects the conservation of angular momentum and parity in the subprocess.

As shown in Figure 2(d), the dependence of the differential cross section on the photon rapidity y has a maximum at y=±1.95 and decreases with decreasing absolute value of rapidity y. The differential cross section is minimal when y=0.

Figure 2(e) shows that the $d\sigma/dx_T^2$ differential cross section decreases rapidly with

increasing x_T, indicating suppression of gluon and photon production with large transverse momenta. This is consistent with theoretical predictions based on pQCD, which show that the cross section is proportional to $\alpha_s\alpha$, where α_s is the tight coupling constant and α is the fine structure constant. Since α_s and α are small, the cross section is expected to be small for large x_T. Figure 2(e) also shows that the dependence of the differential cross section on x_T is not linear, but has a power-law character. This is due to the fact that the cross-section is sensitive to the quark and antiquark PDFs, which describe the probability of finding a parton with a given fraction of the proton momentum. The PDFs are not constant, but vary depending on the fraction of the momentum and the energy scale of the process. In general, the PDFs decrease with increasing momentum fraction, reflecting the fact that there are fewer partons with high momenta inside the proton.

b. Differential cross-section of subprocess of annihilation of quark-antiquark pair $q\bar{q} \to g\gamma$ at collision of longitudinally polarized protons

Figure 3(a,b,c,d,e) shows the dependences of the differential cross sections calculated taking into account the longitudinally polarization of protons on the sum of the energy of colliding particles $\sqrt{s}$, the transverse momentum of prompt photons p_T, the cosine of the scattering angle of prompt photons, the rapidity y and x_T at $\sqrt{s}$=10 GeV.

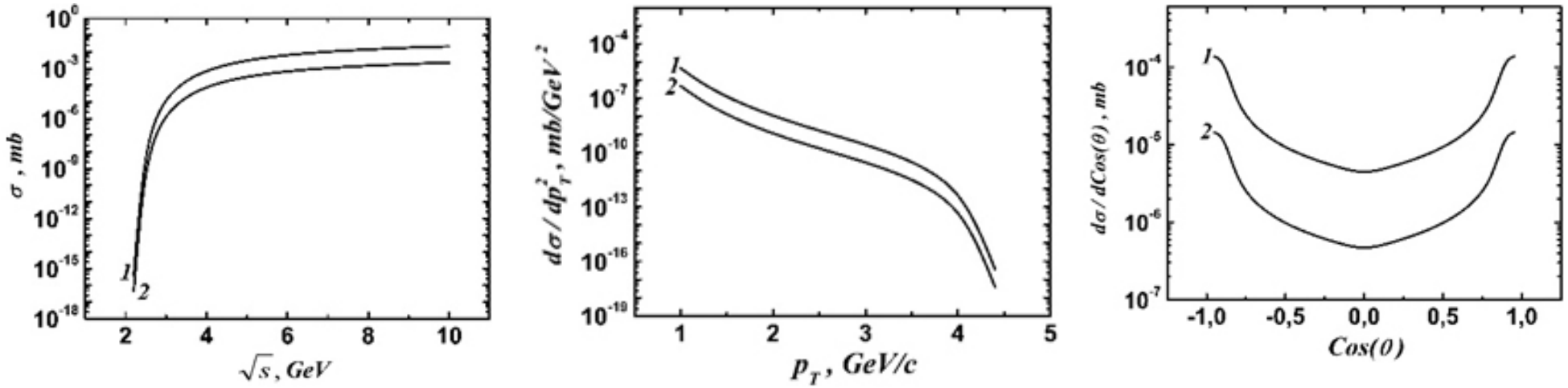

a *b* *c*

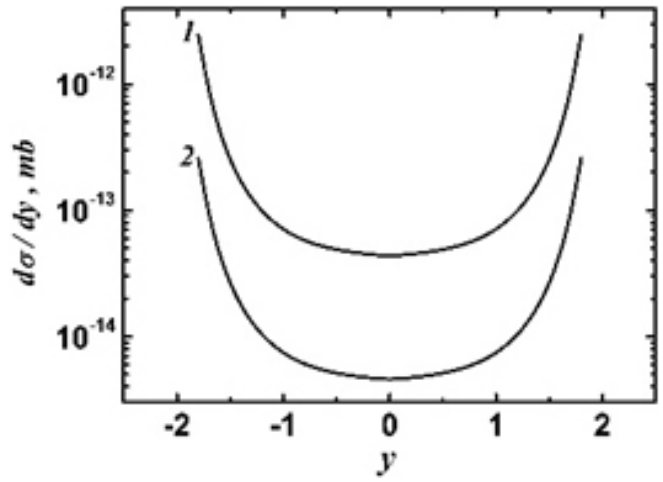

d

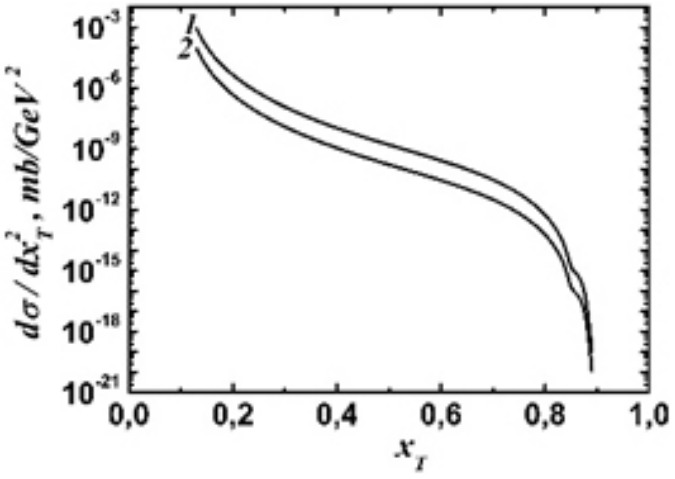

e

Fig.3(a,b,c,d,e) Dependence of the differential cross section of the subprocess $q\bar{q} \to g\gamma$ taking into account the polarization of colliding protons, calculated in the NLO at P_1, P_2=0.9, -0.9 (curve 1) and at P_1=P_2=±0.9 (curve 2) on the sum of the energy of colliding particles $\sqrt{s}$ (a), the transverse momentum of prompt photons p_T (b), the cosine of the scattering angle of prompt photons (c), the rapidity y (d) and x_T (d) at $\sqrt{s}$=10 GeV

From the dependencies in Figure 3(a,b,c,d,e) it is evident that polarization does not affect the character of the dependencies. With opposite polarization the differential cross-section increases, and with the same polarization it decreases, which is similar to

the LO.

From Figure 3(a) it is evident that in the considered range of changes in the energy of colliding protons, the total cross sections σ of the subprocess increase with an increase in the sum of the energies of the colliding particles $\sqrt{s}$.

The differential cross section of the subprocess decreases rapidly as the transverse momentum p_T of prompt photons increases (Figure 3(b)).

The dependence of the differential cross section $d\sigma/dCos(\theta)$ on the cosine of the scattering angle Cos(θ) has a symmetrical pointed shape with a maximum at Cos(θ)=±1 and a minimum at Cos(θ)=0 (Figure 4(c)).

The differential cross-section has a maximum at y=±1.95 and decreases with a change in y, reaching its minimum at the point y=0 (Figure 3(d)).

Figure 4 shows a 3-D graph of the dependence of the doublespin asymmetry of the quark-antiquark pair annihilation subprocess calculated in the NLO on the polarization order P_1 and P_2 of the colliding particles.

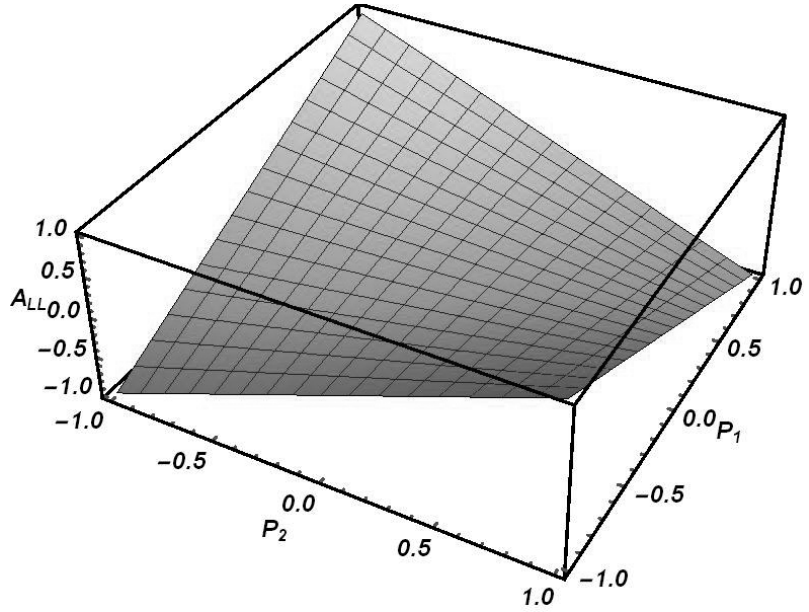

Fig.4 3-D graph of the dependence of the doublespin asymmetry of the annihilation subprocess of the quark-antiquark pair $q\bar{q} \to g\gamma$ on the polarization order P_1 and P_2 of the colliding particles at $\sqrt{s}$=10 GeV.

Maximum positive asymmetry, $A_{LL} \approx +1.0$ is achieved when the polarizations P_1 and P_2 have the same sign and maximal magnitude (i.e., $P_1 = P_2 = 1$ or $P_1 = P_2 = -1$). Physically, this implies that the reaction cross-section $\sigma(q \uparrow \bar{q} \uparrow) \gg \sigma(q \uparrow \bar{q} \downarrow)$. In other words, the annihilation process is most probable when the quark and antiquark spins are aligned parallel to each other (either both along or both against their direction of

motion). This is a direct consequence of the spin structure of the QCD and QED interaction vertices, specifically the helicity selection rules.

Maximum negative asymmetry, $A_{LL} \approx -1.0$ is observed when the polarizations have opposite signs ($P_1 = 1,\ P_2 = -1$, or vice versa). In this scenario, the cross-section $\sigma(q \uparrow \bar{q} \downarrow) \gg \sigma(q \uparrow \bar{q} \uparrow)$, and the process favors an antiparallel spin configuration.

The asymmetry vanishes, A_{LL}=0 if at least one of the initial particles is unpolarized ($P_1 = 0$ or $P_2 = 0$). This is a natural consequence, as the absence of polarization implies no preferred spin direction and, therefore, no possible asymmetry.

c. Comparison of differential cross sections annihilation of quark-antiquark pair $\boldsymbol{q\bar{q} \rightarrow g\gamma}$ *calculated in LO and NLO at collision of nonpolarized proton*

The contribution of the NLO to the differential cross section was determined by studying the dependence of the ratio $R = \frac{d\sigma_{NLO}(q\bar{q}\rightarrow g\gamma)}{d\sigma_{LO}(q\bar{q}\rightarrow g\gamma)}$ on the sum of the energy of

colliding particles $\sqrt{s}$ and the transverse momentum of prompt photons p_T at $\sqrt{s}$=10 GeV.

Figure 5(a,b) shows the dependence of the ratio $R = \frac{d\sigma_{NLO}(q\bar{q}\to g\gamma)}{d\sigma_{LO}(q\bar{q}\to g\gamma)}$ on the energy of colliding protons and the transverse momentum of prompt photons p_T at $\sqrt{s}$=10 GeV.

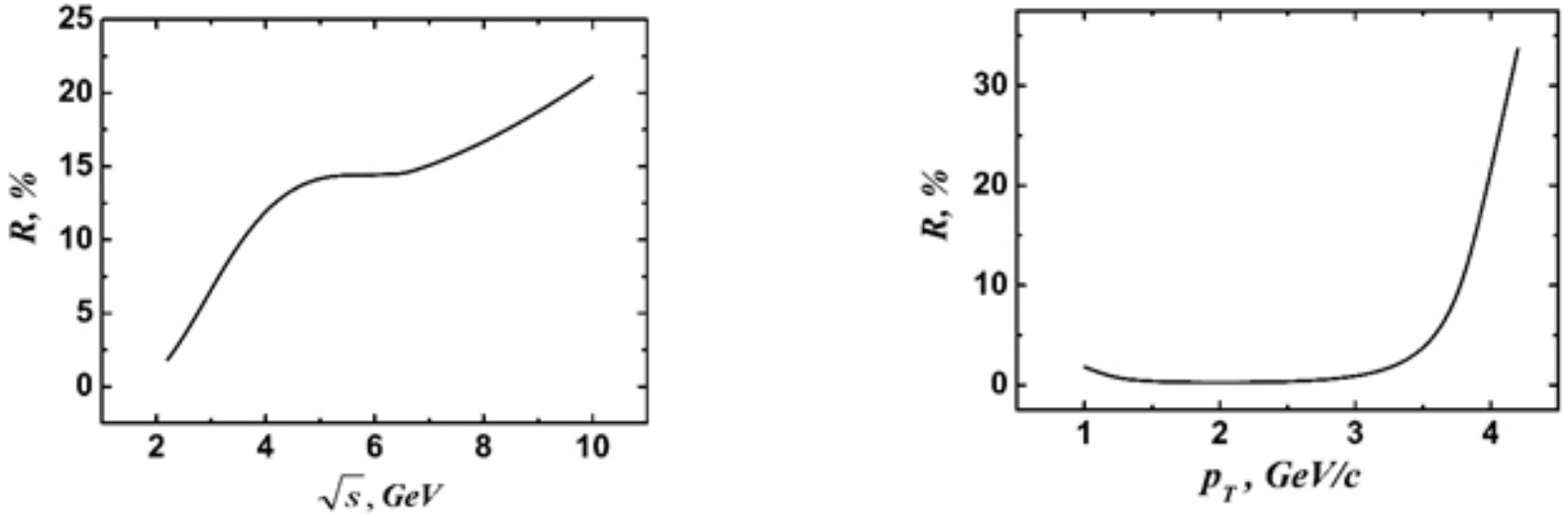

a *b*

Fig.5(a,b) Dependence of the ratio $R = \frac{d\sigma_{NLO}(q\bar{q}\to g\gamma)}{d\sigma_{LO}(q\bar{q}\to g\gamma)}$ on the energy of colliding particles $\sqrt{s}$, transverse momentum of promptt photons p_T (b) at $\sqrt{s}$=10 GeV

As can be seen from Figure 5(a), as the value of $\sqrt{s}$ increases in the [2. 10] GeV range, the value of R increases, which shows the importance of taking into account the NLO calculations at high energies of $\sqrt{s}$.

The dependence of R on the transverse momentum of prompt photons p_T shows that the contribution of the NLO corrections reaches up to 30% at large transverse momenta of prompt photons p_T (Figure 5(b)).

Comparing the contributions of the LO and NLO, one can see that the LO contribution is proportional to $\alpha_s\alpha$, while the NLO contribution is proportional to $\alpha_s^2\alpha$. NLO calculations include additional Feynman diagrams and higher-order corrections. Increasing the number of Feynman diagrams in the NLO means including more complex and virtual particle exchanges, which leads to a more accurate description of the physical process. The interference term is proportional to $\alpha_s^2\alpha\, log(s/M^2)$, where M is the renormalization scale. The interference term changes sign at $s \approx M^2$, leading to a minimum in the cross section. The NLO also includes terms proportional to

$\alpha_s^2\, log(p_T^2/M^2)$,, which increase as p_T increases. The cross section also increases as the values of the DF increase at small *x*. Therefore, NLO calculations can yield a differential cross section contribution that is smaller than that predicted by the LO.

d.Comparison of differential cross sections annihilation of quark-antiquark pair $q\bar{q} \rightarrow g\gamma$ *calculated in LO and NLO at collision of longitudinally polarized proton*

Figure 6(a,b) show the ratios $R = \frac{d\sigma_{LO_{pol}}(q\bar{q}\rightarrow g\gamma)}{d\sigma_{LO}(q\bar{q}\rightarrow g\gamma)}$ and $R = \frac{d\sigma_{NLO_{pol}}(q\bar{q}\rightarrow g\gamma)}{d\sigma_{NLO}(q\bar{q}\rightarrow g\gamma)}$ on the sum of the energies of the colliding particles $\sqrt{s}$.

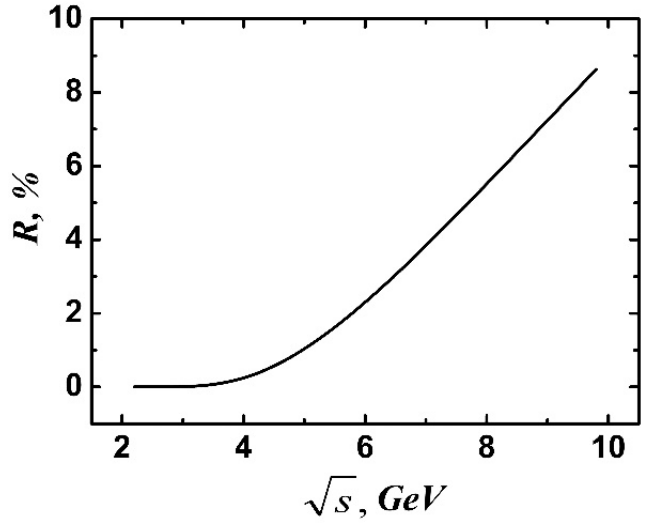

a

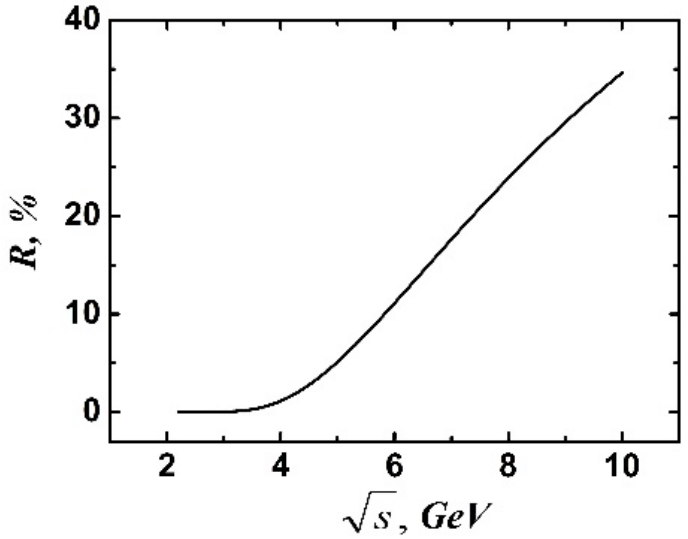

b

Fig.6(a,b) Dependence of the ratios $R = \frac{d\sigma_{LO_{pol}}(q\bar{q}\to g\gamma)}{d\sigma_{LO}(q\bar{q}\to g\gamma)}$ and $R = \frac{d\sigma_{NLO_{POL}}(q\bar{q}\to g\gamma)}{d\sigma_{NLO}(q\bar{q}\to g\gamma)}$ on the sum of the energy of colliding particles $\sqrt{s}$

As can be seen from Figure 6(a,b) as the sum energy of colliding particles increases $\sqrt{s}$, an increase in the effect of polarization in the LO and NLO is observed. It can be seen from the differential cross sections of the LO and NLO for the quark-antiquark pair annihilation subprocess $q\bar{q} \to g\gamma$ that the longitudinally polarization of proton strongly

influences the NLO than the LO. The contribution of the calculation to the NLO on the differential cross section is significant at high energies of the colliding particles.

The reason for this may be: firstly, new Feynman diagrams appear in NLO calculations that include corrections for the virtual loop. These new diagrams often produce contributions with opposite signs compared to the LO diagrams, resulting in a decrease in the overall cross-section of the process. However, for specific observable quantities such as polarization asymmetry, this suppression may not be as effective, leading to a stronger relative influence of the remaining polarization-sensitive terms. Second, NLO calculations account for additional kinematic configurations compared to LO, including higher order parton scattering and gluon emission. These configurations may be more sensitive to proton spin orientation, resulting in greater polarization dependence compared to the more constrained kinematic pattern in LO.

CONCLUSIONS

Presented calculations showed the significant of NLO calculations for the more accurate description of prompt photon production in annihilation of quark-antiquark pair in proton-proton collision.

The dependence of differential cross-section on sum of energy of colliding protons $\sqrt{s}$ calculated in NLO is significant at large values of energy $\sqrt{s}$.

The difference between the differential cross-sections calculated at LO and NLO is small at low and high transverse momentum p_T.

The photon has a high probability of production along the collision axis of proton (angles are 16 and 164 degrees).

From the dependences of ratio $R = \frac{d\sigma_{NLO}}{d\sigma_{LO}}$ on the sum of the energies of the colliding initial particles $\sqrt{s}$, the transverse momentum p_T of the prompt photons, the cosine of the scattering angle $Cos(\theta)$, the rapidity y and x_T of the prompt photons it can be seen that

the NLO corrections increasingly affect the description of the process. The differential cross sections of annihilation of quark-antiquark pairs calculated by the NLO are about 30% of the calculations performed in the LO. This corresponds to pQCD, in which the higher-order terms give larger radiative corrections at higher energies of the partons.

The longitudinal polarization of colliding protons does not change the character of the dependence of the differential cross sections of the subprocesses of quark-antiquark pair annihilation on kinematic parameters. The longitudinal polarization of colliding particles affects the values of the differential cross sections of quark-antiquark pair annihilation. The same polarization direction of colliding particles, the differential cross section of the subprocesses of annihilation of quark-antiquark pairs decreases. Polarization of colliding particles strongly influences the subprocess of annihilation of quark-antiquark pairs. The influence of proton polarization on the differential cross section is indicated by the interaction of parton spins.

Annihilation of a quark-antiquark pair is a strong process associated with color charge. The influence of polarization during annihilation is due to the conservation of angular momentum.

Polarization is significant at small p_T for annihilation of quark-antiquark pair $q\bar{q} \rightarrow g\gamma$.

Comparison of our calculations in NICA energies with NLO calculations carried out at the LHC and the American Tevatron energies showed that the NLO is approximately 15% and 35% of LO for the NICA and LHC, American Tevatron energies, correspondingly [20].

The results obtained indicate the need to take into account NLO contributions when simulation and analyzing experimental data on the process of prompt photon production in proton-proton collisions at NICA and FAIR energies.

---

[20] Klasen, M. Prompt photon production and photon-jet correlations at the LHC / M. Klasen, C. Klein-Bösing, H. Poppenborg // J. High Energy Phys., – 2018. 03, – p. 1-22.

THANK YOU FOR YOUR ATTENTION

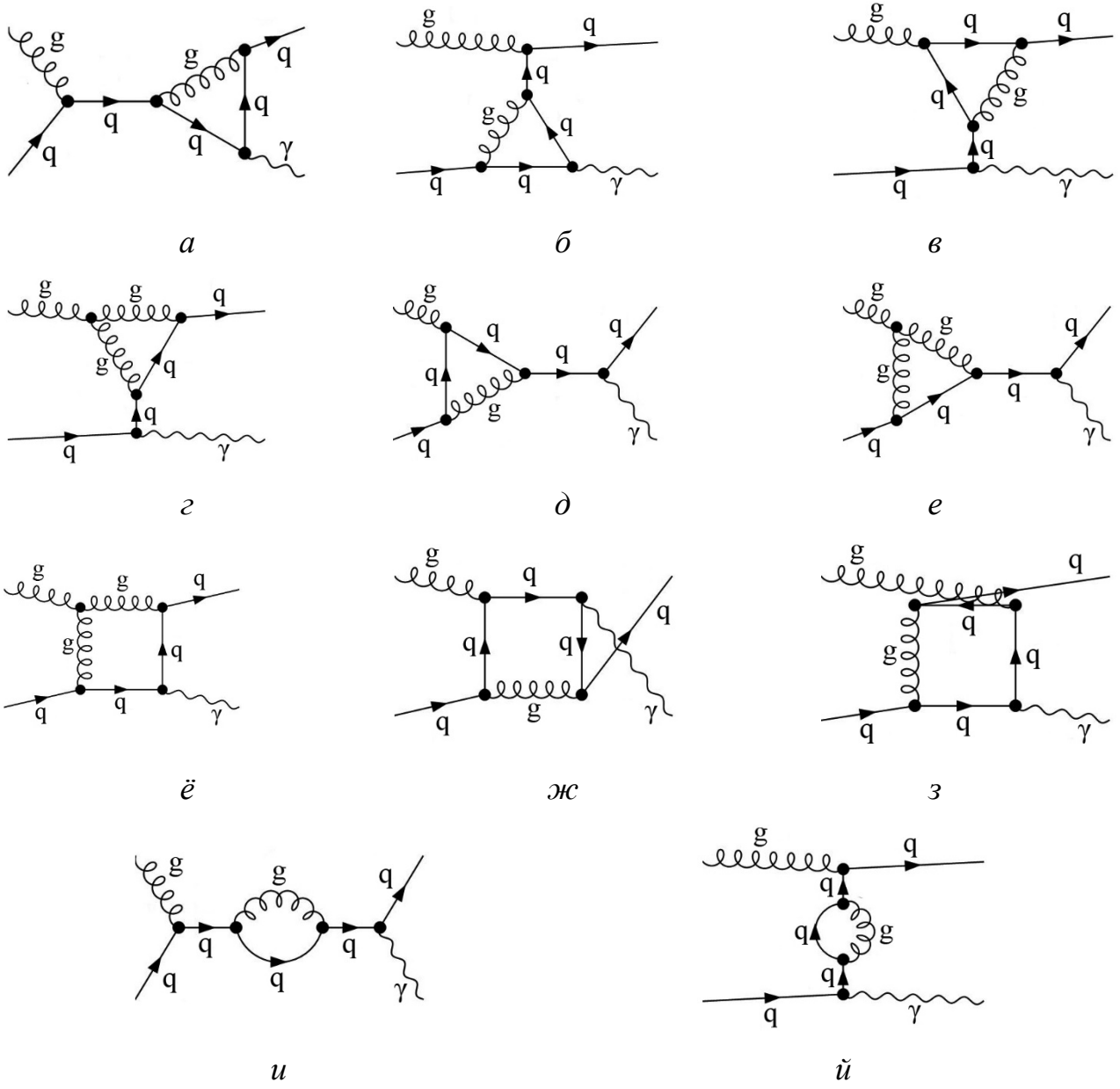

Рисунок 3.1.1(а,б,в,г,д,е,*ё*,ж,з,и,й). Диаграммы одна петлевой коррекции для подпроцесса смешанного комптоновского рассеяния кварк-глюона $qg \to q\gamma$